AFRL-RD-PS-
TR-2018-0006

DYNAMICS OF THE EMISSION FROM A LIGHT FILAMENT

Jean-Claude Diels

Center for High Technology Materials
Univeristy of New Mexico
1313 Goddard SE
Albuquerque, NM 87106

30 Jan 2018

Technical Report

AIR FORCE RESEARCH LABORATORY
Directed Energy Directorate
3550 Aberdeen Ave SE
AIR FORCE MATERIEL COMMAND
KIRTLAND AIR FORCE BASE, NM 87117-5776

NOTICE AND SIGNATURE PAGE

Using Government drawings, specifications, or other data included in this document for any purpose other than Government procurement does not in any way obligate the U.S. Government. The fact that the Government formulated or supplied the drawings, specifications, or other data, does not license the holder or any other person or corporation; or convey any rights or permission to manufacture, use, or sell any patented invention that may relate to them.

This report was cleared for public release by the AFMC Public Affairs Office and is available to the general public, including foreign nationals. Copies may be obtained from the Defense Technical Information Center (DTIC) (`http://www.dtic.mil`).

AFRL-RD-PS-TR-2018-0006 HAS BEEN REVIEWED AND IS APPROVED FOR PUBLICATION IN ACCORDANCE WITH ASSIGNED DISTRIBUTION STATEMENT.

//Andreas Schmitt-Sody//	//Stephen Langdon//
ANDREAS SCHMITT-SODY, DR III	STEPHEN LANGDON, DR III Branch Chief, HPEM Technologies Branch

This report is published in the interest of scientific and technical information exchange, and its publication does not constitute the Government's approval or disapproval of its ideas or findings.

REPORT DOCUMENTATION PAGE

Form Approved
OMB No. 0704-0188

1. REPORT DATE *(22-01-2018)*	**2. REPORT TYPE**	**3. DATES COVERED** *(From - To)*
30-01-2018	Technical Report	01-06-2015 to 30-01-2018

4. TITLE AND SUBTITLE

Dynamics of the Emission from a Light Filament

5a. CONTRACT NUMBER

5b. GRANT NUMBER
FA9451-15-1-0039

5c. PROGRAM ELEMENT NUMBER

6. AUTHOR(S)
Jean-Claude Diels

5d. PROJECT NUMBER

5e. TASK NUMBER

5f. WORK UNIT NUMBER
D08W

7. PERFORMING ORGANIZATION NAME(S) AND ADDRESS(ES)
University of New Mexico
Center for High Technology Materials
1313 Goddard SE
Albuquerque, NM 87106

8. PERFORMING ORGANIZATION REPORT NUMBER

9. SPONSORING/MONITORING AGENCY NAME(S) AND ADDRESS(ES)

Air Force Research Laboratory
3550 Aberdeen Ave SE
Kirtland AFB, NM 87117-5776

10. SPONSOR/MONITOR'S ACRONYM(S)

AFRL/RDHP

11. SPONSOR/MONITOR'S REPORT NUMBER(S)
AFRL-RD-PS-TR-2018-0006

12. DISTRIBUTION/AVAILABILITY STATEMENT
APPROVED FOR PUBLIC RELEASE: DISTRIBUTION IS UNLIMITED

13. SUPPLEMENTARY NOTES

Government Purpose Rights. AFMC PA Number AFMC-2018-0315

14. ABSTRACT

This report covers a basic research program on the propagation of ultrashort pulses of high intensity in air. After the optical beam collapses because of the lensing the high intensity induces in air, a balance between self-focusing and electron plasma defocusing takes place which confines the beam over a long distance, compensating diffraction. Movies are created, following at the speed of light the 2-dimensional image of the radiation, trapped in its self-made waveguide of "filament". Attempt is made to add another dimension to this movie: the wavelength of the radiation that is followed. The signal - divided among space coordinates, time and wavelength is unfortunately below a detectable level. Eliminating one space dimension, a time delay is measured for the first time between the exciting laser pulse and the emission of the nitrogen cation. This indicates clearly a light emitting molecular positive ion is not produced at the time of ionization by a femtosecond pulse.

15. SUBJECT TERMS
Ultrashort pulses; Filaments, High intensity; Air lasing

16. SECURITY CLASSIFICATION OF:			**17. LIMITATION OF ABSTRACT**	**18. NUMBER OF PAGES**	**19a. NAME OF RESPONSIBLE PERSON**
a. REPORT	**b. ABSTRACT**	**c. THIS PAGE**			Andreas Schmitt-Sody
UNCLASSIFIED	UNCLASSIFIED	UNCLASSIFIED	SAR	22	**19b. TELEPHONE NUMBER** *(include area code)*

This page intentionally left blank.

TABLE OF CONTENTS

LIST OF FIGURES

Figure **Page**

1.0 SUMMARY

For light pulses of sufficient intensity, even air is a nonlinear medium. Femtosecond pulses of a few mJ in the near infrared have sufficient intensity not only to self-focus in air, but also to maintain a very small (of the order of 250 μm) diameter over distances longer than the Rayleigh range, a phenomenon called *filamentation*. Other nonlinear effects include multi-photon ionization, emission of an annular rainbow of colors in the far field dubbed "conical emission", and amplified spontaneous emission of particular transitions of the nitrogen cation N_2^+. This emission is of particular interest because the presence of optical gain can lead to "lasing in air". Air lasing propagates in the forward and backward directions, opening the prospect of atmospheric interrogation through remote Raman spectroscopy (using the air lasing line as a pump). Despite three decades of research in this field, there are still numerous basic questions unanswered. The questions addressed in this report are:

1. Is a filament really a self-induced waveguide, or an artifact due to a "moving focus" (a self-focus is intensity dependent, thus time dependent) or axicon focusing (a square or super-Gaussian spatial beam profile produces a line of foci)

2. What is the mechanism producing optical gain in the nitrogen cation? Can we measure

   (a) if the gain is produced in the femtosecond duration of the exciting/ionizing 800 nm pulse?

   (b) if the gain lives long enough to produce a reasonable gain length?

   (c) a delay between the ionizing optical pulse and the emission of the nitrogen cation.

We solved item (1) by creating a movie of the propagating pulse with the streak camera. The movie was obtained by imaging a very small section of the filament produced at 10 Hz onto the streak camera, and stepping that section after each shot along the propagation direction. Each frame of the streak camera records light intensity versus time and one spatial coordinate. The other coordinate is stepped from shot to shot. The movie is produced by computationally re-organizing the data into two dimensional (y, z) pictures at successive time steps. The movie showed indeed the filamented light pulse moving at the speed of light while remaining confined in the transverse dimension.

To unravel the mechanism of emission by the nitrogen cation, the first approach was to produce a 4-dimensional video: two spatial coordinates, spectrum, and time. This is a particularly challenging task, because:

1. The number of photons available is divided among all four dimensions

2. Difficulties of synchronization and the limited temporal resolution of the streak camera

3. Shot to shot pulse energy fluctuation of the laser operated at 10 Hz

4. Statistical variations of the filament starting point.

Attempts to make 4D movies were made, using a prism arrangement to display the spectrum. This approach was unsuccessful because of low signal strength. However, the goal or time resolving the side emission of the nitrogen cation was successfully realized. Shot to shot pulse fluctuations were eliminated operating by the laser at 1 kHz. The pulses were 50 fs in duration, and 1 mJ energy. The data acquisition rate was still limited to 10 Hz by the time required to process/upload each frame. Optical synchronization was improved by directing a weak reference pulse into the streak camera. The timing of the laser pulse with respect to the reference was determined independently using Rayleigh scattering from small and diluted aerosols produced by a nebulizer, and confirmed by using a solid diffusing target. The statistical fluctuations of the starting point were eliminated either using an aerodynamic window (which was verified not to introduce any distortion of the beam), or preparing the filament with a 10 cm focal distance lens. Filters were used to select the emission line to be investigated.

The emission of the **B** $\rightarrow$ **X** transition of the nitrogen cation was determined to occur 32 ps after the 800 nm pulse in the case of the $\nu = 0 \rightarrow \nu = 1$ transition near 428 nm, and 39 ps in the case of the $\nu = 0 \rightarrow \nu = 0$ transition near 391 nm. The emission lifetime is on the order of 40 ps.

It is the first time that the cation emission has been time resolved from the exciting short pulse. However this new finding adds more questions to the complex mechanism of nitrogen emission, and calls for more theoretical and experimental investigation.

2.0 INTRODUCTION

The objective of this work is to gain a better understanding of the propagation of intense fs light pulses in air, as they collapse in a self-induced waveguide or filament. In particular we want to time resolve the emission associated with the light matter interaction that has created the waveguiding. Light filaments [1, 2] contain confined regions of high intensity and can trigger various nonlinearities leading in particular to optical gain. “Air lasing” [3] or superradiance can be exploited for Raman probing of the atmosphere in forward and backward directions. High resolution pump-probe spectroscopy has revealed very complex mechanism by which optical gain arises at various vibrational-rotation transitions in the cation N_2^+ [4]. One element missing in this complex puzzle is the initial timing: when and where in the filament is the N_2^+ generated, and when does it start emitting?

3.0 METHODS, ASSUMPTION AND PROCEDURES

To help observing and understanding filaments in air, a new technique of creating a “video” of the moving light pulse and the plasma emission in its wake was devised. The motion is captured by making successive pictures of the (repetitive) pulse at stepped location. Such technique applied only to repetitive events that can be exactly synchronized. The moving

object to be “filmed” is imaged onto the entrance slit of a streak camera. 2D snapshots in time-space are recorded as the point of observation is scanned. In the snapshot, time resolution is achieved along the axis orthogonal to the streak camera slit, and a spatial dimension is recorded along the slit. A second spatial dimension orthogonal to the slit is scanned with an optical system. The laser pulses are 50 fs in duration, 30 mJ energy, at a repetition rate of 10 Hz.

3.1 The Technique

3.1.1 Setup

In the setup sketched in Figure 1, the slit of a streak camera is located at the image plane of the object (the filament). Radiation composed of rayleigh scattering at the fil-

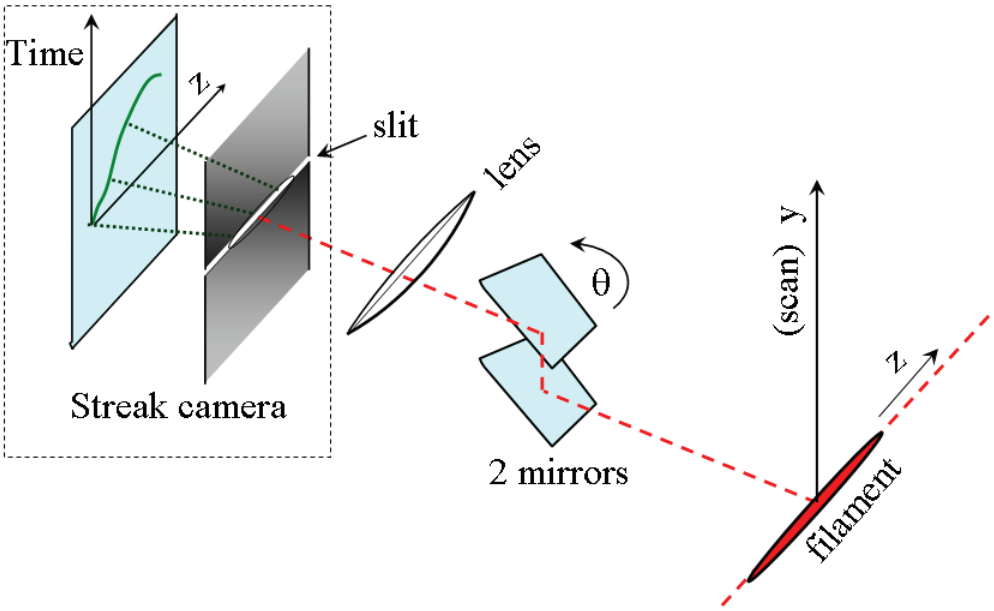

Figure 1: Experimental Setup. The Camera System Observes Light Emitted Transversally by the Filaments.

ament wavelength, but also fluorescence light at various wavelengths from the ions and molecules excited in the wake of the filament is captured. The slit of the streak camera selects the real image of a line approximately parallel to the filament axis. The light is relayed by two large UV enhanced aluminum mirrors, one of which can be rotated. The real image of the filament is moved from shot to shot across the slit with the rotating mirror. The angle θ is scanned over 6 mrad in 200s or 1000s, time during which 200 or 1000 streak camera images are recorded. Each frame contains the space time information along a line of the filament. An individual streak camera image covers a single row of pixels. Images are continuously captured while the field of view is scanned across the filament by rotating a relay mirror, at a Slow enough rate to rnsure continuity in the transverse dimension. The individual images are then computationally organized in two dimensional (y, z) pictures in successive time steps to provide a video .The light is relayed via a periscope made of

two large UV enhanced aluminum mirrors. In the arrangement of the figure, the slit of the camera is parallel to the propagation axis z of the filament. With the streak camera being triggered when the filamented pulse is in the field of view of the camera, the frame displays light intensity versus time z (a line along the filament). Each frame is a recording of the light collected along the slit, versus time. Images are continuously captured while the field of view is scanned along y by rotating a relay mirror, at a slow enough rate to ensure continuity in the longitudinal dimension. The individual images are then computationally organized by two dimensional (y, z) pictures in successive time steps to provide a video.

3.2 Filaments Produced With 3 m Focusing at 10Hz

3.2.1 Focusing in Air

Filaments are typically launched with lenses of longer focal length, about 3 m. One data set is presented in Figure 2 for focusing in air. Frames Are separated by 2.88 ps. selected frames are shown between Frame 1 to 100. For later frames an average over 100 frames is shown to reduce noise. The intensity averaged over a 100 pixel x 100 pixel array around the middle of the filamentation region was selected to generate a plot of radiated intensity versus time [Figure 2 (b)]. It shows a plasma risetime of 90 ps and a fall time of 200 ps.

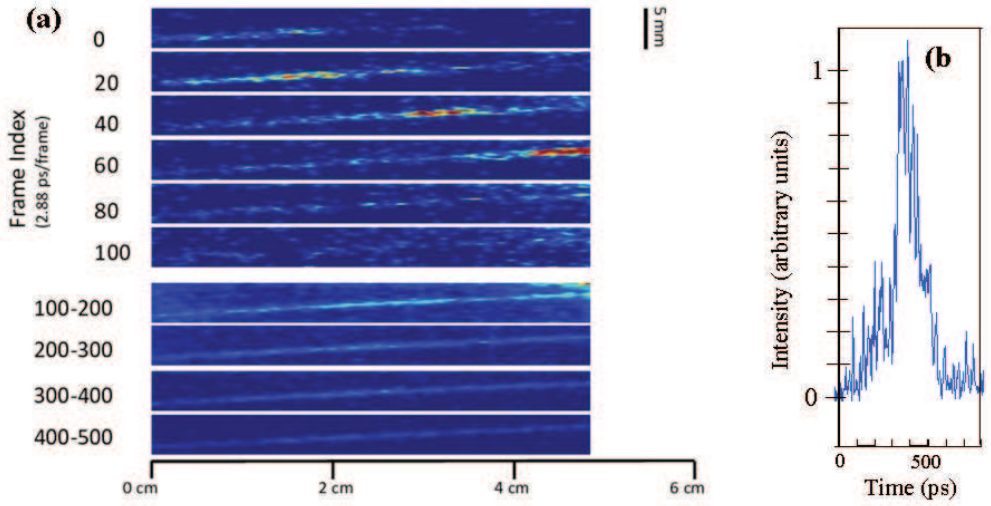

Figure 2: (a) Filament of a 800nm Pulse Using Long Focal Length in Air With Unfiltered Detection. (b) Intensity of the Radiation Versus Time.

3.2.2 Focusing in Vacuum

The length of the trace representing the plasma in Figure 2 may not be representative of the true plasma length if there is a jitter in the starting point of the filament (along z). To ensure that the starting point of filaments in air is repeatable, the pulses are focused in vacuum onto the 2 mm transition region vacuum-atmosphere of an aerodynamic

window [5]. In this configuration the filament is created at the exit of the window in atmospheric air. Using this method the shot to shot generation of plasma and filament is well aligned in the three dimensional space. Selected frames of the reconstructed movie are shown in Figure 3 (a). The emission is indeed shorter (along z) and brighter. The plasma emission is plotted in Figure 3 (b). The reduced jitter enables a better resolution with a 40 ps rise time and 230 ps fall time (both times being measured from 10% to 90%).

The transverse dimension of the plasma is smaller compared to in air focusing. This is explained in Section 4.0 where we measured the beam pointing stability through the aerodynamic window (Figure 6).

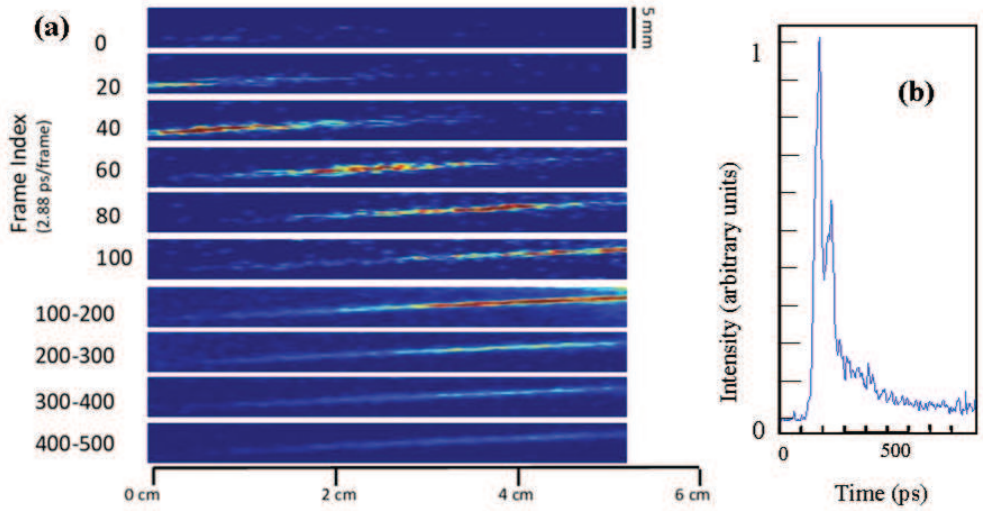

Figure 3: Filament of a 800nm Pulse With Unfiltered Detection, Focused With 3 Meter focal Length Lens in Vacuum Through an Aerodynamic Window. (b) Intensity of the Radiation Versus Time.

4.0 CHALLENGES AND NEW APPROACH

Our prior work on the filament movie indicates a delay between the filament and the plasma emission [6]. This delay could not be identified directly on the movie, or on the selected frames of Figure 3(a). Time integration of the data of that figure along a vertical line around the position at 2 cm shown in Figure 3 was interpreted as a Raleigh scattering peak followed by the emission. The efforts in this program were directed at achieving sufficient resolution in time and spectrum to identify the process leading to N_2^+ emission.

4.1 Instrumental Jitter Elimination

There are three elements that determine the time resolution of the system:

1. The accuracy of positioning the frames with respect to each other
2. The intrinsic resolution of the streak camera

3. The reproducibility of the event under observation

a. Optical synchronization of frames

There is 60 nanosecond delay between trigger and sweep of the streak camera. Therefore, one can not use the same laser pulse to trigger the camera for the same frame. The streak camera is triggered electronically through the master clock of the laser system, thereby inheriting the jitter of the laser electronics. The accuracy of optical timing is transferred to each image by using a reference optical beam. A reference optical beam is selected from the same pulse that creates the filament and sent through a fixed path directly to the camera. The path of the reference beam is such as to illuminate always a point of the photocathode in the time frame of the camera streak, providing a temporal reference for every streak camera image. Mechanical and electronic jitter between frames are corrected by using the timing of the reference pulse in the reconstruction code. The streak camera is provided with a fiber to make a synchronization spot on the photocathode. The synchronization was tested by imaging simultaneously weak scattering on the photocathode. This experiment determined that the signal through the fiber had an unacceptable width. Best results were obtained with the arrangement of Figure 4.The dashed line is the synchronization beam split off the main beam. It is sent onto the streak camera through the connector hole intended for the synchronization fiber.The optical paths are adjusted such that the pulse on the dashed line reaches the photocathode at the same time of the signal scattered from the filament

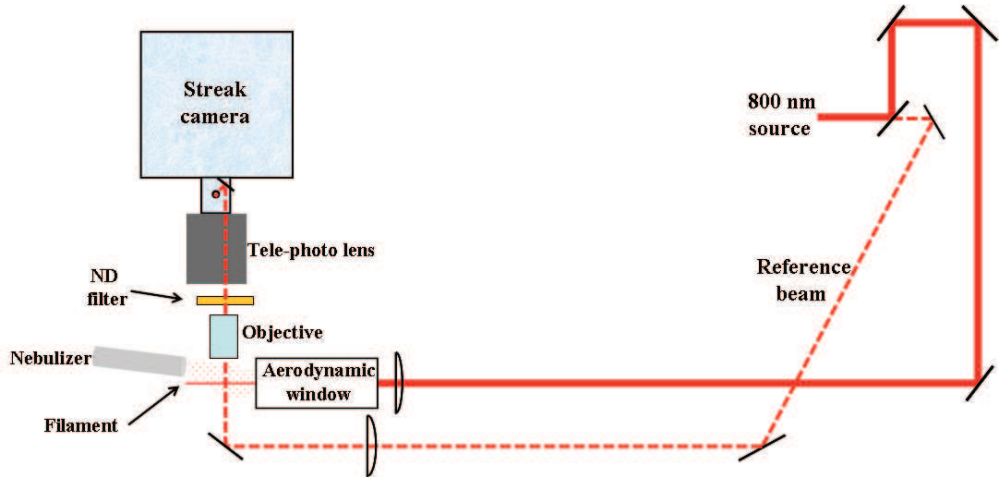

Figure 4: Sketch of the Detection System and Synchronization.

b. Intrinsic resolution of the streak camera

For these data, we need the best temporal resolution the streak camera can provide. The response to a delta function light pulse, obtained by scattering the filament off a diffuser, is extremely sensitive to the slit opening. In fact, it is only with the slit opened to its minimum (i.e. closed) that we achieve the resolution quoted by the manufacturer.

The signal is then so weak that it is reduced to a few scattered dots. In order to achieve the best resolution, it is necessary to average between 1000 and 2500 frames. In doing so, the frames have to be synchronized as discussed in the previous paragraph. The intensity of the synchronization pulse should also be such that there be only 0 to 20 pixels irradiated per frame (10 to 20 electrons on the entrance face of the MCP. The algorithm used is to take the average of all the synchronization dots, excluding those that are outside an area 4 $\times$ the mean square deviation. This average is take as reference of all frames. Figure 5 shows a image of a scatterer (1000 frames are averaged). Both reference point

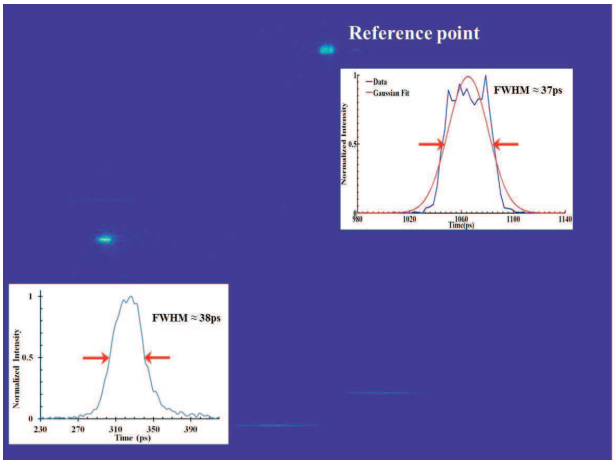

Figure 5: Typical Average of 1000 Frames, Recording the Scattering of a Diffuser. For Ideal Resolution, the Reference (Top) And the Image Have the Same Intensity. Note That They Also Have the Same Width

and image have the same width of 38 ps. This picture indicates that we can define the centroid and the middle of the leading edge with an precision of a few ps.

c. Reproducibility of the event under observation

The laser used in reference [6] at a repetition rate of 10 Hz had a poor shot-to-shot reproducibility. In all data to follow, laser operation at 1 kHz is used, which has considerably better pulse to pulse reproducibility. When the filament is prepared by focusing the beam with a long focal length [3 m in the case of Figure 2], the plasma appears with a width of 290 ps. This low resolution is attributed to the jitter in starting point of the plasma. This jitter is eliminated by the use of an aerodynamic window as can be seen by comparing Figure 2 with Figure 3, the latter having a two times shorter risetime. A surprising observation is the brighter and narrower emission in the case of the filament created with the beam focused in vacuum. This feature was explained by measuring the beam pointing stability of a He-Ne beam sent through the same path, either in air (aerodynamic window not activated) or in vacuum through the aerodynamic window. The results is shown in Figure 6 where the centroid and the beam size of a He-Ne beam transmitted through the aerodynamic window is plotted as a function of time.The turquoise and violet plots pertain to the x (Horizontal) and y (Vertical) axis, respectively, when the beam is propagated in air (Aerodynamic Window Inoperative). The green and dark blue pertain to x (Horizontal)

and y (Vertical) axis, respectively, when the beam is propagated through vacuum, with the aerodynamic window operated. Clearly the fluctuation in position and width of the He-Ne beam are *reduced* when sending the He-Ne beam in vacuum through the aerodynamic window. This is consistent with the slight increase in brightness and reduced width observed in Figure 3 as compared to Figure 2.

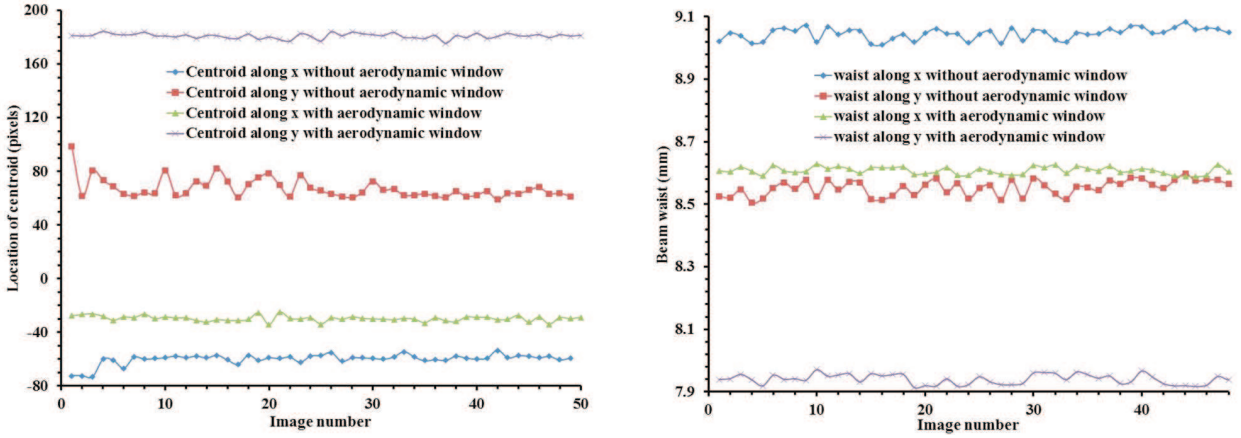

Figure 6: Test Showing the Absence of Beam Distortion by Operating the Aerodynamic Window. The Centroid of the Image (Left) And the Beam Size (Second Order Moment) are Plotted as a Function of Time.

4.2 Light Collection Efficiency and Spectral Resolution

The emission of a single filament is very weak, the plasma density being typically of the order of 10^{16} cm^{-3}. The total signal is further decreased by the fact that we attempt to measure a number of photon emitted per picosecond, and per unit transverse and longitudinal coordinate. One of the most difficult challenges to address is to collect as efficiently as possible all the light that is emitted radially. The initial experiments [7] were using a 10 cm diameter 60 cm focal distance lens to image the filament. The signal to noise was very poor.

In an attempt to collect more light from the filament, a 10 cm diameter mirror of short focal distance (10 cm) was used in the configuration of Figure 8 (Section 5.1). The light signal could not be resolved.

To optimize the collection efficiency, numerous configurations were attempted, using a spectrometer instead of the streak camera. Best results were obtained by starting the filament with a 10 cm focal distance lens, and imaging the filament onto the horizontal slit of the spectrometer with a long working distance 20x microscope objective. While numerous spectra were take with high resolution for the 391 nm and 428 nm emission of N_2^+ *on axis*, all attempts failed to observe these lines with the 800 nm filament. To verify that we could observe these lines from the side of a filament, we switched to the UV filament produced by a 200 mJ, 170 ps pulse at 266 nm. In this configuration we were able to record for the first time, from the side of a filament, the spectrum of the nitrogen cation near 391 and 428 nm, as shown in Figure 7. These spectra are usually seen only

along the axis of the beam, seeded by the second harmonic of the fundamental [4]. It is not clear whether what is observed is spontaneous emission or scattering from the amplified emission seeded by the conical emission of the filament. For the transition between vibrational levels $\nu = 0$ from the **B** state to the $\nu = 0$ of the ground **X** state at the wavelength range around 391 nm, no difference with beam prepared in air or vacuum. The **R** branch is slightly more intense when the beam has been focused in vacuum through the aerodynamic window for the $\nu = 0 \rightarrow \nu = 1$ transition around 428 nm. In both cases, the emission is weak with circularly polarized beam of the same intensity. This is expected since the field is reduced by a factor $\sqrt{2}$ for circular polarization versus linear of the same intensity.

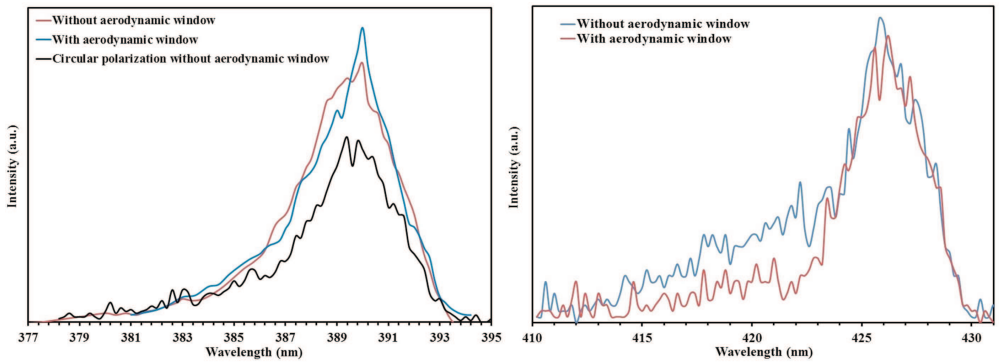

Figure 7: B $\rightarrow$ X Emission of the Nitrogen Cation No Difference is Seen between the Emission With (Blue) or Without (Red) Aerodynamic Window (Linear Polarization). Black Curve: Emission for Circular Polarization. Right: Emission From the $\nu = 0 \rightarrow \nu = 1$ Transition Near 428 nm. A Slight Increase in the R Branch is Seen Between the Emission With (Blue) or Without (Red) Aerodynamic window.

5.0 RESULTS AND DISCUSSION

5.1 Attempts at 4D Movies

The initial ambitious goal was to produce a 4 dimensional movie: filament intensity versus transverse and longitudinal coordinate, as a function of propagation time and wavelength. In order to disperse the spectrum with maximum efficiency we chose dispersion by prisms in the optical configurations of Figure 8. In the case of Figure 8(a), the filament is imaged through the two 10 cm long prisms onto the slit of the streak camera. The slit is oriented in the plane of the figure. Each frame will record a spectrum (versus the slit direction) versus time. Similar to the arrangement in Figure 1, a setup with two mirrors would scan the frames along the z direction (axis of the filament). In the case of Figure 8(b), two mirrors are used to scan the spectrum orthogonally to the slit direction. The longitudinal (z) dimension is imaged directly along the slit.

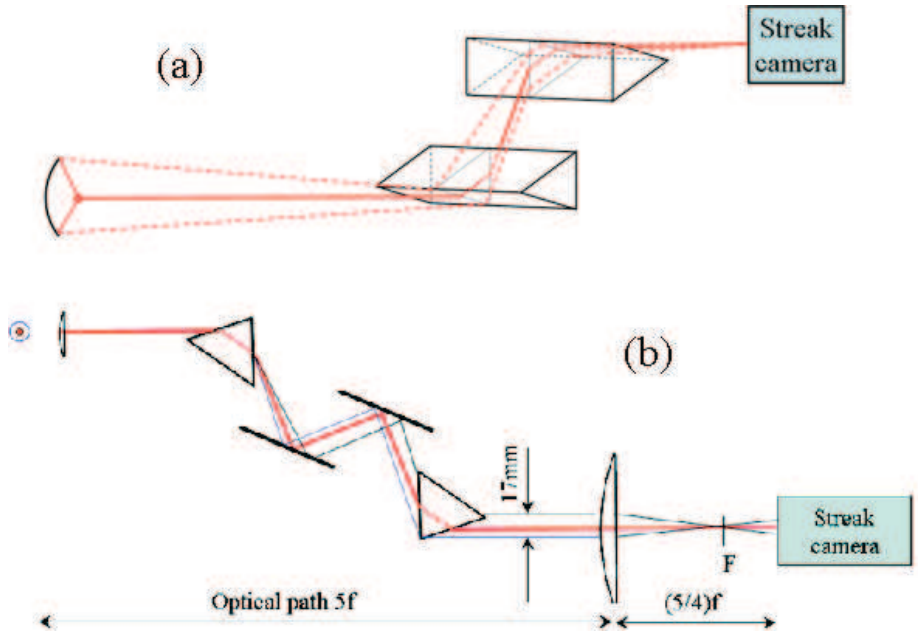

Figure 8: Attempts to Introduce Spectral Resolution to Extend to 4D the 3D Visualization of Filaments Previously Demonstrated

5.2 Absolute Timing of the Nitrogen Cation Emission

Rayleigh scattering at 800 nm from air molecules is too weak to be observed (and time resolved) with the streak camera. Since we have achieved accurate timing of each frame with the reference pulse as demonstrated in Figure 4 and 5,] we can perform independent measurements to determine the arrival time of the 800 nm with respect to the reference, and another series of measurements to record the time dependence of the emission. The problem is to be ascertain with precision that exactly the same spot is being observed in both experiments. Using a diffuser plate — such as was done in the experiment to determine the instrumental resolution — puts one at the mercy of an error in positioning. The solution that we chose to use Rayleigh scattering enhanced by aerosols. The aerosols are blown through the camera field of view along the path of the filament.

The challenge here is to create droplets that enhance scattering without creating plasma and/or producing and optical resonances [8] in the droplet. The solution chosen is to produce droplets of the order of 1 μm diameter with a nebulizer (mist generator based on Bernoulli principle). These droplets were sufficiently small as not to create any visible plasma or local illumination. The reference point was accurately determined by recording Rayleigh scattering of the lowest density mist.

Data taken to time resolve the various plasma are corrected for the time delay introduced by any filter inserted before the streak camera. The reference is the Rayleigh scattering of the laser enhanced by a minimum of mist from the nebulizer [Figure 9(a)] which will be used in the whole series of measurements. For the sweep speed of 100ps used in all the data presented below, each pixel is 2.8767 ps.

The relative delays in the emissions at 391 nm and 428 nm are shown in Figure 10. As mentioned previously, there is not enough emission to get a high resolution spectrum

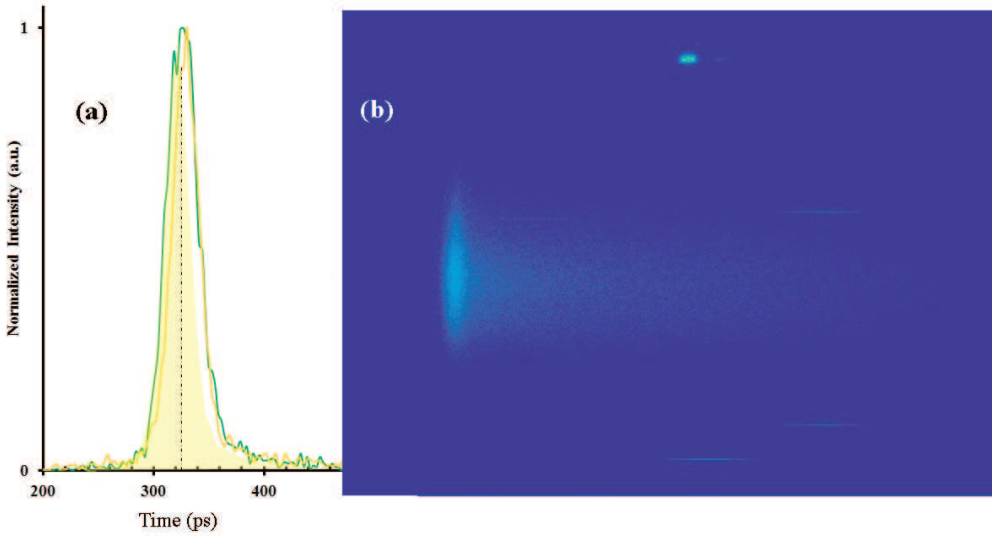

Figure 9: (a) In Yellow: the Reference Pulse Obtained by Sending the Laser Beam Through a Very Dispersed Mist. Green: Reference Pulse Obtained With a Solid Diffuser Surface. The Dashed Line Indicating the Center of Gravity of the Yellow Reference Will be Used as the Time of Arrival of the fs Pulse. (b) Typical Streak Camera Frame

resolving every rotational line as in reference [4]. Instead, The spectral regions were selected with square "brightline" single band Semrock filters centered at 427 nm and 390 nnm. Figure 10(a) shows the emission around 428 nm, following the Rayleigh reference (in yellow), as a function of time in ps. Figure 10(b) shows the emission around 391 nm, following the Rayleigh reference (in red), as a function of time in ps. These curves (a) and (b) are normalized. The recordings of Figure 10(c) are not normalized, to indicate the relative intensities. The dashed-dotted line indicate the timing of the exciting fs pulse. The 428 radiation is slightly more intense than the 391 nm. The times of arrival are 32 ps and 39 ps after the fs pulse, for the 428 nm and 391 nm emission, respectively.

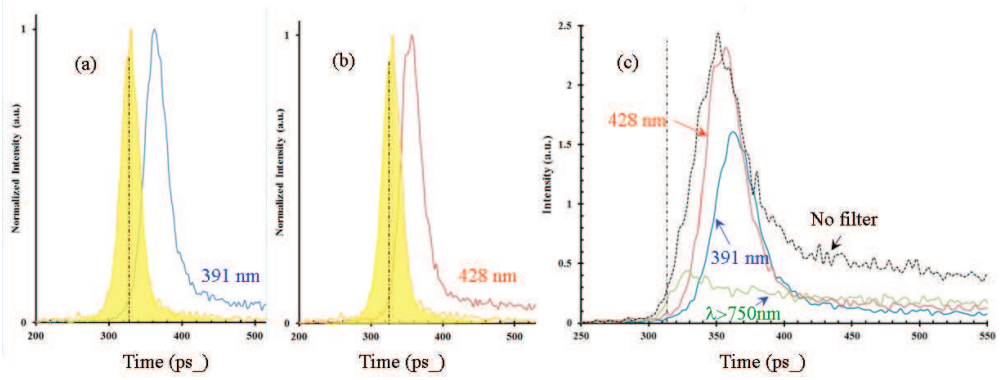

Figure 10: Time Resolved Filament Emission. (a) And (b) Show the (Normalized) Time Resolved Emission of the Nitrogen Cation at 391 nm (Blue) and at 428 nm (Red). The Yellow Profile is the Rayleigh Scattering From the Exciting Pulse at 800 nm.

It is surprising that the N_2^+ radiation is not produced at the time of ionization. The 30

ps delay may involve collisions, or a decay of the N_2^+ from a higher state to the **B** state. Possibly the intense pulse could first dissociate N_2, ionize the atom to form N^+, which would thereafter create the excited N_2^+ with the observed 30 ps delay.

The emission lifetime is on the order of 40 ps. This is much shorter than the 240 ps and 800 ps measured for the **P** and **R** branches, respectively in high resolution spectroscopy of the nitrogen cation emission at 100 torr [4]. The difference is to be attributed to collision broadening at atmospheric pressure, and that the measurements of [4] were taken in a pure nitrogen cell. The lifetime is however much shorter than the 130 ps reported by Xu *et al.* [9].

The complete emission over all range of wavelengths is the dashed black line in Figure 10(c). It is much longer lived, and starts earlier than the cation emission. With a long pass filter at 750 nm, some radiation is observed simultaneously with the laser, and a slow decay [green curve in Figure 10(c)].

It is the first time that the cation emission has been time resolved from the exciting short pulse. This new finding adds to more unresolved questions surrounding the mechanism of nitrogen emission, and calls for more theoretical and experimental investigation.

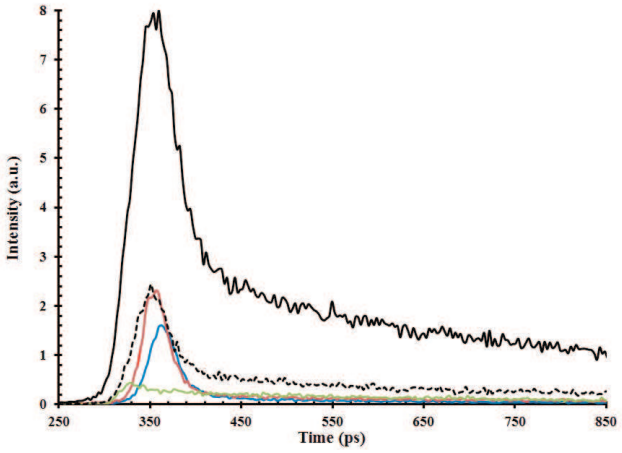

Figure 11: Time Resolved Filament Emission, Not Normalized. The Blue, Red And Green Lines Correspond to the Wavelengths $\lambda = 391$ nm, 428 nm and $\lambda \geq 750$ nm, Respectively. The Black Curve Shows Radiation Collected Without Any Filter, With the Same Slit Opening Than for the Other Signals.

6.0 CONCLUSIONS

This project aims at a better understanding of the propagation of intense ultrashort light pulses in the atmosphere, their interaction with nitrogen molecules, and the blue emission from these molecules. The light energy appears to confine itself in a filament, a filiform cylindrical volume of the order 100 μm diameter extending for distance of the order of meters, beyond the expected Rayleigh range for this wavelength (800 nm) and transverse dimension. One controversial point is whether the light energy is spread along this line as a nonlinear focal point moves towards and from the source, or as can be caused by nonlinear axicon focusing, or if the pulse energy remains concentrated and propagates in a self-made waveguide. This point has been resolved through the use of a streak camera to create a movies of the propagating pulse. In these movies one can see the filament being a light pulse moving at the speed of light, while remaining confined in the longitudinal and transverse dimension.

The temporal and spatial resolution of the initial experiment was marred by the poor spatial and temporal resolution due mainly to large energy fluctuations of the 10 Hz source of ultrashort pulse, the uncertainty about the starting point of the filament, the extreme weakness of the signal and imperfect synchronization of the camera and light. All these elements have been considerably improved, with the goal of making 4-dimensional movies of the moving filament and the radiation propagating in its wake. The 4 dimensions were two spatial co-ordinates, spectrum, and time. A prism arrangement was used to disperse the spectrum with maximum visibility. Still this approach was unsuccessful mainly due to the fact that the signal reaching the streak camera was too low.

The goal of time-resolving the initiation of the nitrogen cation emission is however successfully realized in the next set of experiments. The filament is created by laser pulses of 50fs duration at 800nm with an energy of 1mJ, and at a repetition rate of 1 kHz. The high pulse rate is needed to have highly reproducible pulses. It does not reduce the measurement time, which is set by the processing time of the streak camera, limiting the data acquisition rate to 10 Hz.

The timing of the laser pulse with respect to the reference is determined independently using Rayleigh scattering from small and diluted aerosols produced by a nebulizer, and confirmed by using a solid diffusing target. The statistical fluctuations of the starting point are eliminated either using an aerodynamic window (which was verified not to introduce any distortion of the beam), or preparing the filament with a 10 cm focal distance lens. Filters are used to select the emission line to be investigated. Rather than being simultaneous with the 800 nm ultrashort pulse, the emission of the $\mathbf{B} \rightarrow \mathbf{X}$ line of the nitrogen cation is seen to be delayed by 32 ps for the $\nu = 0 \rightarrow \nu$ = 1 transition near 428 nm, and 39 ps in the case of the $\nu = 0 \rightarrow \nu$ = 1 transition near 391 nm. The lifetime of both emissions is of the order of 40 ps.

It is the first time that the cation emission has been time resolved from short pulse laser excitation. This new finding adds to more unresolved questions surrounding the mechanism of nitrogen emission, and calls for more theoretical and experimental investigation.

7.0 REFERENCES

[1] A. Braun, G. Korn, X. Liu, D. Du, J. Squier, and G. Mourou, "Self-channeling of high-peak-power femtosecond laser pulses in air," *Optics Lett.*, vol. 20, pp. 73–75, 1995.

[2] X. M. Zhao, P. Rambo, and J.-C. Diels, "Filamentation of femtosecond UV pulses in air," in *QELS, 1995*, vol. 16, (Baltimore, MA), p. 178 (QThD2), Optical Society of America, 1995.

[3] Q. Luo, W. Liu, and S. L. Chin, "Lasing action in air induced by ultra-fast laser filamentation," *Appl. Phys. B*, vol. 76, pp. 337–340, 2003.

[4] L. Arissian, B. Kamer, and J.-C. DIels, "Ultrafast dynamics of N_2^+ emission in strong laser field," *J. of physics B*, vol. submitted, 2018.

[5] J.-C. Diels, J. Yeak, D. Mirell, R. Fuentes, S. Rostami, D. Faccio, and P. di Trapani, "Air filaments and vacuum," *Laser Physics*, vol. 20, pp. 1101–1106, 2010.

[6] A. Velten, A. Schmitt-Sody, S. Rostami, A. Rasoulof, C. Feng, J.-C. Diels, and L. Arissian, "Movies of plasmas and light filaments," *Journal of Physics B: Atomic, Molecular and Optical Physics*, vol. 48, p. 094020, 2015.

[7] A. Velten, A. Schmitt-Sody, and J.-C. Diels, "Precise intracavity phase measurement in an optical parametric oscillator with two pulses per cavity round-trip," *Optics Letters*, vol. 35, pp. 1181–1183, 2010.

[8] H. C. Bryant and N. Jarmie, "The Glory," *Scientific American*, vol. 231, pp. 60–71, 1974.

[9] H. Xu, A. Azarm, J. Bernhardt, Y. Kamali, and S. Chin, "The mechanism of nitrogen fluorescence inside a femtosecond laser filament in air," *Chemical Physics*, vol. 360, pp. 171–175, 2009.

LIST OF SYMBOLS, ABBREVIATIONS, AND ACRONYMS

AFRL	Air Force Research Lab
TR	Tech Report

DISTRIBUTION LIST

DTIC/OCP
8725 John J. Kingman Rd, Suite 0944
Ft Belvoir, VA 22060-6218 1 cy

AFRL/RVIL
Kirtland AFB, NM 87117-5776 1 cy

Official Record Copy
AFRL/RDHP/Andreas Schmitt-Sody, DR III 1 cy